Journal of Magnetism and Magnetic Materials 427 (2017) 34–40

Contents lists available at ScienceDirect

Journal of Magnetism and Magnetic Materials

journal homepage: www.elsevier.com/locate/jmmm

Magnetic graphene oxide as a carrier for targeted delivery of chemotherapy drugs in cancer therapy

Ya-Shu Huang[a], Yu-Jen Lu[b], Jyh-Ping Chen[a,c,d,e,*]

[a] Department of Chemical and Materials Engineering, Chang Gung University, Kwei-San, Taoyuan 33302, Taiwan, ROC
[b] Department of Neurosurgery, Chang Gung Memorial Hospital, Kwei-San, Taoyuan 33305, Taiwan, ROC
[c] Department of Plastic and Reconstructive Surgery and Craniofacial Research Center, Chang Gung Memorial Hospital, Kwei-San, Taoyuan 33305, Taiwan, ROC
[d] Graduate Institute of Health Industry and Technology, Research Center for Industry of Human Ecology, Chang Gung University of Science and Technology, Kwei-San, Taoyuan 33302, Taiwan, ROC
[e] Department of Materials Engineering, Ming Chi University of Technology, Tai-Shan, New Taipei City 24301, Taiwan, ROC

ARTICLE INFO

Keywords:
Magnetic nanoparticles
Magnetic graphene oxide
Doxorubicin
Irinotecan
Drug delivery

ABSTRACT

A magnetic targeted functionalized graphene oxide (GO) complex is constituted as a nanocarrier for targeted delivery and pH-responsive controlled release of chemotherapy drugs to cancer cells. Magnetic graphene oxide (mGO) was prepared by chemical co-precipitation of Fe_3O_4 magnetic nanoparticles on GO nano-platelets. The mGO was successively modified by chitosan and mPEG-NHS through covalent bindings to synthesize mGOC-PEG. The polyethylene glycol (PEG) moiety is expected to prolong the circulation time of mGO by reducing the reticuloendothelial system clearance. Irinotecan (CPT-11) or doxorubicin (DOX) was loaded to mGOC-PEG through π-π stacking interactions for magnetic targeted delivery of the cancer chemotherapy drug. The best values of loading efficiency and loading content of CPT-11 were 54% and 2.7% respectively; whereas for DOX, they were 65% and 393% The pH-dependent drug release profile was further experimented at different pHs, in which ~60% of DOX was released at pH 5.4 and ~10% was released at pH 7.4. In contrast, ~90% CPT-11 was released at pH 5.4 and ~70% at pH 7.4. Based on the drug loading and release characteristics, mGOC-PEG/DOX was further chosen for in vitro cytotoxicity tests against U87 human glioblastoma cell line. The IC50 value of mGOC-PEG/DOX was found to be similar to that of free DOX but was reduced dramatically when subject to magnetic targeting. It is concluded that with the high drug loading and pH-dependent drug release properties, mGOC-PEG will be a promising drug carrier for targeted delivery of chemotherapy drugs in cancer therapy.

1. Introduction

One of the research areas in nanomedicine is dedicated to the diagnosis or treatment of disease with nanocarriers that could be modified by different methods to provide a safe and effective cell-targeting function. It is expected that nanocarriers carrying drugs or genes will have potential clinical applications for cancer treatment [1]. The tumor vasculature is frequently immature, disorganized, and chaotic, consisting of loosely fitted endothelial cells lacking pericyte support. Poorly developed leaky vasculature allows 10–100 nm sized nanoparticles to extravasate and gets accumulated with in solid tumor. This enhanced permeability and retention (EPR) effect attributed to the leaky tumor vasculature is considered as a boon for drug-delivery systems with nanocarriers [2,3].

With its low molecular weight, a chemotherapy drug for cancer treatment could be easily accumulated in various tissues during blood circulation, which may lead to severe side effects. The concept of magnetic targeted drug delivery could overcome this difficulty by using magnetic nanocarriers as drug carrier; the drug-loaded magnetic nanocarrier could be quickly guided to the tumor site by a magnetic field to decrease the side effect, after endocytosis by tumor cells [4,5]. Doxorubicin (DOX) has been widely used for cancer chemotherapy. The main mechanism of DOX for cancer cell killing is via chelation of DNA, inhibition of topoisomerase II and the hydroxyl radicals effect [6]. Irinotecan (CPT-11) is a prodrug of SN-38 and a DNA topoisomerase I inhibitor [7]. However, both drugs have severe side effects such as vomiting, nausea, hair loss, tissue inflammation and myocardial injury. Therefore, a functional nanocarrier for targeted delivery of DOX or CPT-11 is very important for cancer therapy. Recently, graphene, a biocompatibility carbon nanomaterial contains sp^2 hybridized carbon

* Corresponding author at: Department of Chemical and Materials Engineering, Chang Gung University, Kwei-San, Taoyuan 33302, Taiwan, ROC.
E-mail address: jpchen@mail.cgu.edu.tw (J.-P. Chen).

http://dx.doi.org/10.1016/j.jmmm.2016.10.042
Received 26 June 2016; Received in revised form 5 October 2016; Accepted 8 October 2016
Available online 10 October 2016
0304-8853/

atoms in a 2-D structure and with a thickness as low as of one atom has been proposed for drug delivery [8–10]. For this purpose, graphene is usually modified to become graphene oxide (GO), by reducing the thickness of GO and increasing the hydrophilic functional groups on GO surface [11]. With the use of π-π stacking and hydrogen bond interactions, a large amount of drug could be adsorbed onto GO due to its large specific surface area. An added advantage of GO for chemotherapeutic drug delivery is the pH-dependent drug release behavior, where enhanced drug release at a low pH value (pH=5.0–5.5) will provide efficient intracellular drug release after endocytosis by the cells for drug release in the endosome [12,13].

In this study, we use magnetic graphene oxide (mGO) for DOX and CPT-11 delivery by preparing mGO through the chemical co-precipitation method [14,15]. As chitosan have excellent properties, such as nontoxicity, biocompatibility, and high positive charge, mGO was modified through covalent binding with chitosan to prepare a positively charged mGO to increase the contact of the nanocarrier with the cell membrane [16]. Chitosan-modified mGO (mGOC) was subsequently grafted with polyethylene glycol (PEG), as PEGlyted mGOC (mGOC-PEG) is expected to avoid the endocytosis by the reticuloendothelial system (RES) and prolong blood circulation of the nanocarrier [17,18]. Hence, we synthesized and characterized mGOC-PEG and investigated drug loading and release of DOX and CPT-11. In vitro cytotoxicity of mGOC-PEG loaded with DOX against U87 cells was tested by magnetic targeting for specific killing of cancer cells, which can substantially reduce the IC50 of the drug.

2. Materials and method

2.1. Preparation of graphene oxide (GO)

Graphene oxide was prepared from graphene based on modified Hummers method. One gram of graphene (N002-PS, Angstron Materials Inc.) was stirred in 23 ml sulfuric acid for 12 h, followed by slowly adding 3 g $KMnO_4$ below 20 °C. The temperature was increased to 40 °C while stirring for another 30 min. The temperature was increased to 80 °C and stirred for another 45 min. 46 ml of double distilled water (ddH_2O) was added and the solution and heated to 98–105 °C for 30 min, followed by cooling down to room temperature for 1 h. Additional ddH_2O (140 ml) and 10 ml of 30% H_2O_2 were added and reacted for 5 min at 40 °C. After the reaction, GO was washed three times with 5% hydrochloride acid by centrifugation and dialyzed against ddH_2O till the pH become neutral. Nano-sized GO was obtained by sonicating for 30 min and filtered with a 0.2 μm filter.

2.2. Synthesis of carboxylated magnetic graphene oxide (mGO)

The mGO was prepared by chemical co-precipitation of Fe_3O_4 magnetic nanoparticles (MNPs) on GO nano-platelets. A solution containing 20 mg GO, 40 mg $FeCl_2{\cdot}4H_2O$ and 108 mg $FeCl_3{\cdot}6H_2O$ (Fe^{2+} and Fe^{3+} ions in 1: 2 molar ratio) in 50 ddH_2O was sonicated for 30 min. The solution was reacted under nitrogen for 30 min and heated to 65 °C. 1 g of chloroacetic acid was added and reacted for 1 h to transform the hydroxyl, epoxide and ester group on GO into carboxylic acid (−COOH) moieties, followed by adding 2 g NaOH and reacted for another 30 min. The mGO was washed with ddH_2O by magnetic separation. The amount of carboxylate groups on mGO was estimated by the toluidine blue O (TBO) method.

2.3. Synthesis of magnetic graphene oxide-chitosan-PEG (mGOC-PEG)

Magnetic graphene oxide-chitosan (mGOC) were prepared by reacting 20 mg m mGO with 500 mg chitosan (molecular weight=9 kDa) in 50 ml MES buffer (pH 6). The mixture was sonicated for 1 h, followed by adding 80 mg 1-ethyl-3-(3-dimethylaminopropyl) carbodiimide hydrochloride and incubated for 24 h at room temperature to form covalent bonds between amine groups of chitosan and carboxylate groups of mGO. The particle was recovered by magnetic separation and washed 3 times with ddH_2O. The amount of amine groups on mGOC was estimated by the 2,4,6-trinitrobenzenesulfonic acid (TNBSA) method. To synthesize mGOC-PEG, mGOC synthesized above was reacted with mPEG-NHS (methoxypolyethylene glycol succinimidyl carbonate ester, molecular weight=2 kDa, Nanocs, USA) for 1 h in ddH_2O by fixing the molar ratio of -NH_2 group in mGOC to the -NHS group in mPEG-NHS to be at 10. mGOC-PEG was recovered by magnetic separation and washed 3 times with ddH_2O water as before.

2.4. Drug loading and drug releasing

Drug loading was determined in 1 ml 0.01 M phosphate buffer containing 0.1 mg mGOC-PEG and different concentrations of DOX or CPT-11. The suspension was rotated at 6 rpm overnight at 4 °C and centrifuged. The amount of loaded drug was calculated from mass balance by determining the concentration of DOX or CPT-11 in the supernatant by a U3010 UV/Vis spectrometer (Hitachi, Japan) at 490 nm and by HPLC, respectively [19]. The drug loading efficiency (%) is defined as (weight of drug loaded on mGOC-PEG/weight of drug initially added) ×100. The drug loading content (%) is defined as (weight of drug loaded on mGOC-PEG/weight of mGOC-PEG) ×100.

For in vitro drug release, 1 mg mGOC-PEG/drug was incubated in 1 ml phosphate buffered saline (PBS, pH=7.4 or pH=5.4) at 37 °C for various times and the whole supernatant solution was removed after magnetic separation. Drug concentration in the supernatant solution was determined as before and the precipitate was re-suspended with 1 ml of fresh PBS of the same pH. The drug release (%) is defined as (weight of drug released/weight of drug loaded on mGOC-PEG) ×100.

2.5. Physico-chemical properties of nanocarriers

The particles size and zeta potential were detected by dynamic light scattering (DLS) using a Zetasizer (Nano ZS 90, Malvern, UK) by diluting the samples to 0.1 mg/ml in ddH_2O. Transmission electron microscope (TEM) observations were conducted using a JEM-2000EXII TEM (JEOL, Tokyo, Japan) at 100 kV. An atomic force microscope (AFM) (Dimension Icon, Bruker, USA) was used to analyze the surface topography, size and thickness of samples. Thermogravimetric analysis (TGA) was determined by TGA 2050 from TA instruments with 8 mg freeze-dried samples in a platinum pan under nitrogen atmosphere from 100 to 700 °C. The nominal gas flow was 60 ml/min and the heating rate was 10 °C/min.

2.6. Cellular uptake of mGOC-PEG/DOX

To determine intracellular uptake of mGOC-PEG, U87 human glioblastoma cells were cultured in 1 ml Dulbecco's Modified Eagle Medium (DMEM) supplemented with 10% fetal bovine serum after seeding in an over slip in a 6-well culture plate (1.0×10^5 cells/well). Cells were grown for 24 h in a humidified CO_2 incubator at 37 °C under 5% CO_2 atmosphere, washed with sterilized PBS 3 times, and incubated with 1 ml mGOC-PEG-carboxylfluorescein/DOX (0.1 mg/ml) suspension for 3 h and analyzed by a confocal laser scanning microscope. The cells nuclei were counterstained with Hoechst 33342 with blue fluorescence. Identifications of mGOC and DOX are possible by the green and red fluorescence signals from fluorescein-labeled mGOC-PEG and DOX, respectively. Possible fluorescence signals from extracellular fluorescein-labeled mGOC-PEG bound to the surfaces of U87 cells were quenched by trypan blue dye solution for 15 min. Since trypan blue is excluded from entering live cells, all fluorescence signals observed will be only from mGOC-PEG taken intracellularly.

2.7. In vitro U87 cells cytotoxicity under magnetic targeting

U87 cells were seeded in 24-well plate (5.0×10^4 cells/well) and cultured for 24 h in a humidified CO_2 incubator at 37 °C under 5% CO_2 atmosphere. The culture plate was placed on a BILATEST™ magnetic separator (Sigma-Aldrich) that consists of a clear Plexiglas block with an extra strong permanent magnets (diameter=7.5 mm) placed at the center of each well. mGOC-PEG/DOX (0.1 mg/ml) was added and cultured for 24 h, followed by PBS washing and staining with a LIVE/DEAD cell viability/cytotoxicity kit for mammalian cells (Thermo Fisher Scientific) and observed under an inverted fluorescence microscope.

2.8. In vitro cytotoxicity of mGOC-PEG/DOX

For in vitro cytotoxicity tests, U87 cells were cultured in DMEM supplemented with 10% fetal bovine serum in a 96-well cell culture plate at a seeding density of 3×10^4 cells/well. The cells were allowed to attach for 24 h. Cells were treated with free DOX in solution, mGOC-PEG/DOX or mGOC-PEG/DOX+magnetic field (with a BioMag® 96-Well Plate Separator from Bangs Laboratories, Inc., USA) at different drug concentrations to determine the IC50 (half-maximum inhibitory concentration) value. Medium in each well was replaced with either mGOC-PEG/DOX suspension or DOX solution prepared in culture medium and incubated in a humidified CO_2 incubator at 37 °C under 5% CO_2 atmosphere. Cell viability after 72 h was determined using MTT assays at 540 nm using a microplate reader. Cell viability using cell culture medium and mGOC-PEG were taken as 100% for DOX and mGOC-PEG/DOX, respectively. Control cytotoxicity experiments to confirm the biocompatibility of the drug-free carrier (mGOC-PEG) were carried out by using U87 cells following the same procedure as described above.

3. Results and discussion

3.1. Preparation of mGOC-PEG

The GO examined by TEM showed flake morphology and the size was ~200–300 nm (Fig. 1A). After chemical co-precipitation of Fe_3O_4 MNPs on GO, mGO had similar size with GO and Fe_3O_4 MNPs could be observed from the TEM image of mGO (Fig. 1B). The AFM images of mGO and mGOC indicated the sheet thickness of mGO was around 12 nm (Fig. 1C), which increased to ~30 nm after modification with chitosan (Fig. 1D). From chemical assays, the amount of carboxylate groups on 1 mg of mGO is 0.487 ± 0.049 μmole while the amine groups on mGOC is 1.797 ± 0.054 μmole.

From Fig. 2A, the average hydrodynamic diameter of GO, mGO, mGOC and mGOC-PEG obtained from DLS ranged from 120 to 200 nm. GO and mGO showed similar size, which increased 50 nm for mGOC after modification with chitosan. However, further modification with PEG did not result in significant increase in particle size. For zeta potentials, GO showed a negative value (−42 mV) due to the abundance of −OH and −COOH. The zeta potential of mGO increased slightly to −37 mV due to the positive charge of Fe_3O_4 MNP (29 mV). Nonetheless, the zeta potential increased dramatically after modified with chitosan (38 mV) due to the abundance of positively charged $-NH_2$ in chitosan. Compared with mGOC, mGOC-PEG shows similar but a lower positive zeta potential (33 mV) as some $-NH_2$ group of chitosan was consumed during the covalent binding step with mPEG-NHS. The highly positive zeta potential of mGOC-PEG could be expected to enhance its contact with the cell surface to increase its endocytosis into the cell.

The composition of the nanocarriers was investigated by TGA in Fig. 3. MNP only showed 3% mass loss from the −OH group on the surface. The GO was thermally unstable and showed significant weight

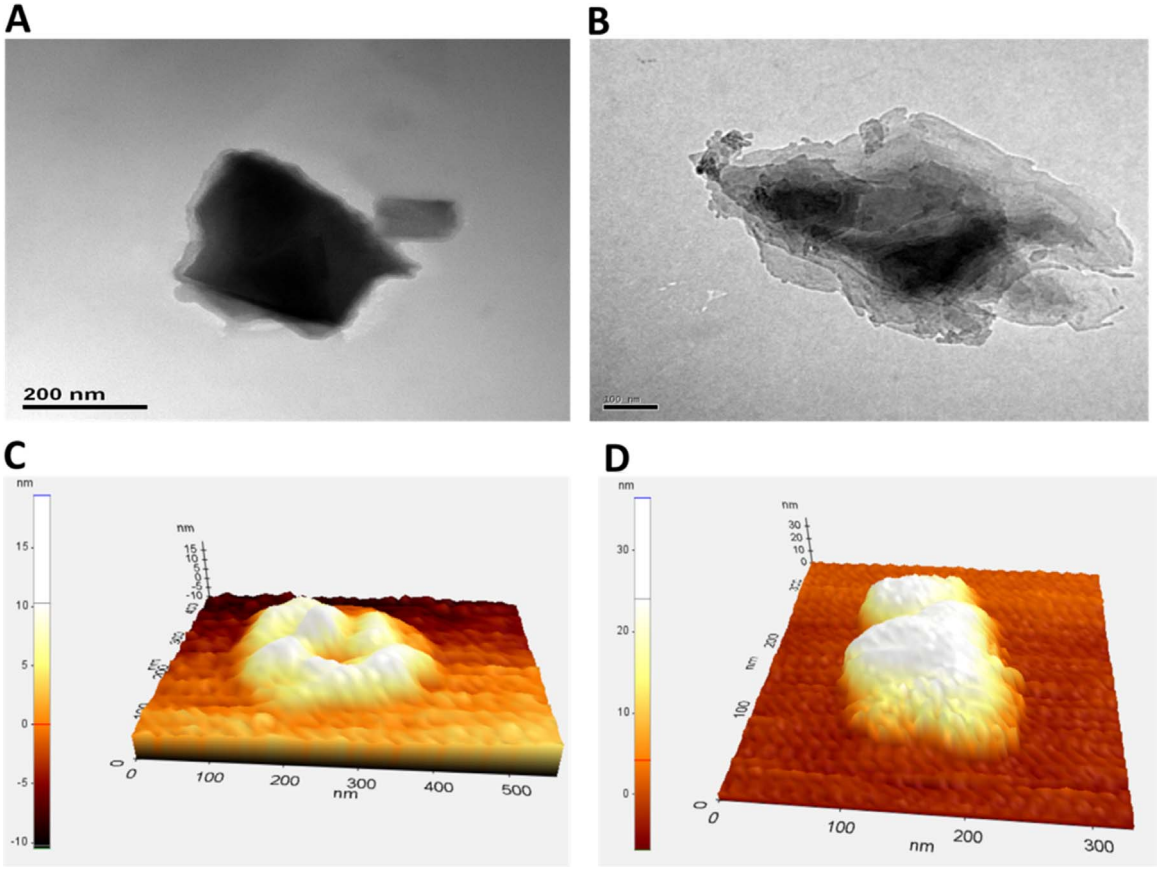

Fig. 1. TEM images of (A) GO (bar=200 nm) and (B) mGO (bar=100 nm). AFM images of (C) mGO and (D) mGOC.

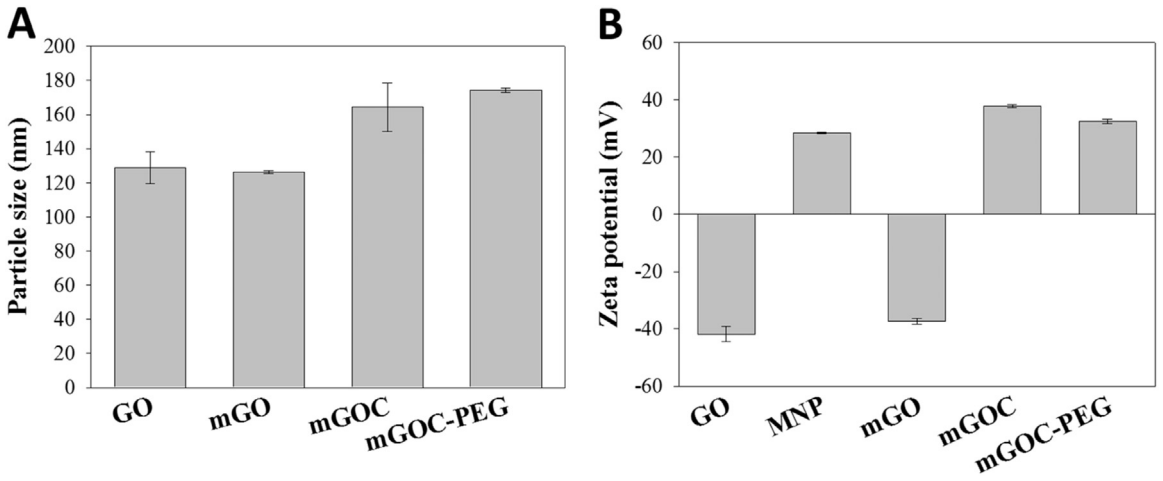

Fig. 2. (A) Particle size by dynamic light scattering and (B) zeta potential of nanocarriers.

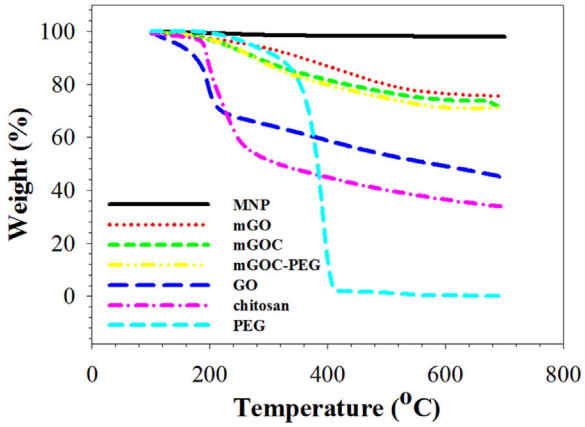

Fig. 3. Thermogravimetric analysis (TGA) of nanocarriers and polymers.

lost from 130 to 250 °C due to the decomposition of the labile oxygen-containing functional groups [20]. The TGA curves of the chitosan showed ~67% weight loss at 700 °C and the thermal pyrolysis was from 200 to 400 °C. The PEG showed ~100% weight loss and the thermal pyrolysis was at 330–400 °C. For mGO after the chemical co-precipitation of MNPs, the thermal pyrolysis was delayed until 210–470 °C and showed less final weight loss compared with GO at ~25%. By calculating the difference in residual weight between GO and mGOC at 700 °C, the mass percentage of MNP in mGO is estimated to be ~30%. The TGA curves for mGOC and mGOC-PEG shows additional weight loss at temperature corresponding to chitosan and PEG respectively, indicating successful covalent modification of mGO with chitosan and PEG. The final weight loss is also consistent with mGOC-PEG > mGOC > mGO as grafted chitosan and PEG will contribute to additional weight loss.

3.2. Drug loading and pH-dependent release from mGOC-PEG

As shown from Fig. 4, the loading efficiency of drug increased with drug concentration while the loading content decreased with drug concentration. Taking both factors into consideration, the best preparation was determined from the intersection of the loading efficiency and loading content curves in Fig. 4. The values of loading efficiency and loading content of CPT-11 were 54% and 2.7% respectively; whereas for DOX, they were 65% and 393% (Fig. 4A and B). The loading efficiency and loading content of DOX is higher than CPT-11, which can be ascribed to different drug chemical structures and resultant π-π stacking interactions with mGOC-PEG. In addition, the $-NH_2$ groups of DOX is expected to form additional hydrogen bindings with mGO.

As π-π stacking and hydrogen binding interaction can be affected by pH change, the pH-dependent drug release profile was further examined at pH 7.4 and 5.3, which correspond to the physiological pH and endosomal pH of cancer cell, respectively. An initial burst release was observed for the drugs during the first 6 h and followed by sustained release up to 120 h. For CPT-11, 90% of the drug was released at pH 5.4 and ~70% was released at pH 7.4. In contrast, ~78% of DOX was released at pH 5.4 and ~17% was released at pH 7.4 (Fig. 5). That the release rate of drug at pH 5.4 is significantly higher than that at pH of

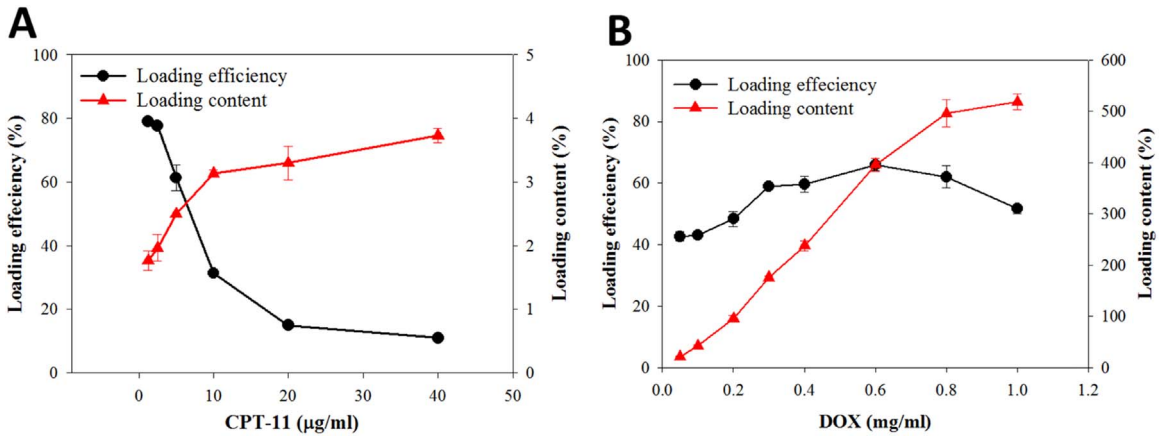

Fig. 4. The drug loading efficiency and drug loading content of mGOC-PEG for CPT-11 (A) and DOX (B).

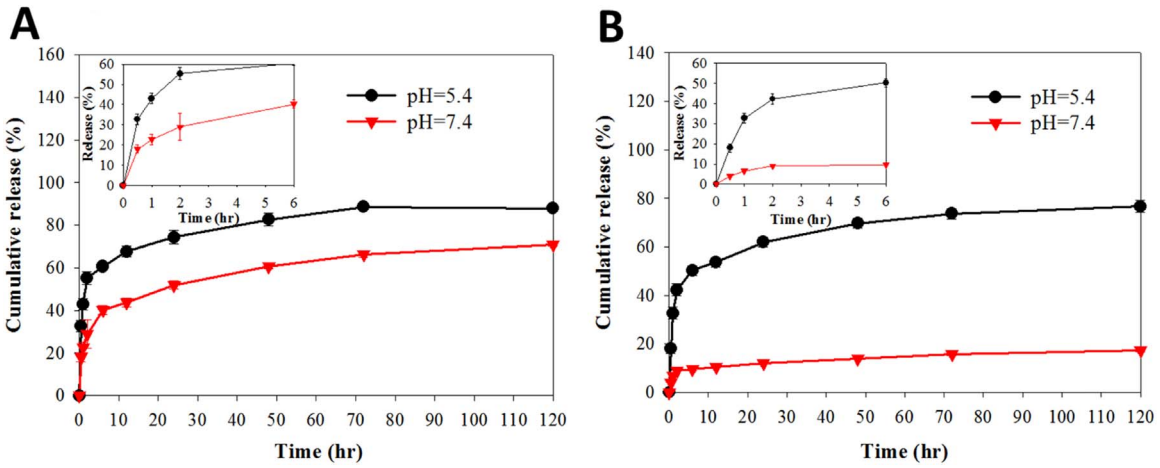

Fig. 5. The pH-dependent drug release profile of CPT-11 (A) and DOX (B) from mGOC-PEG.

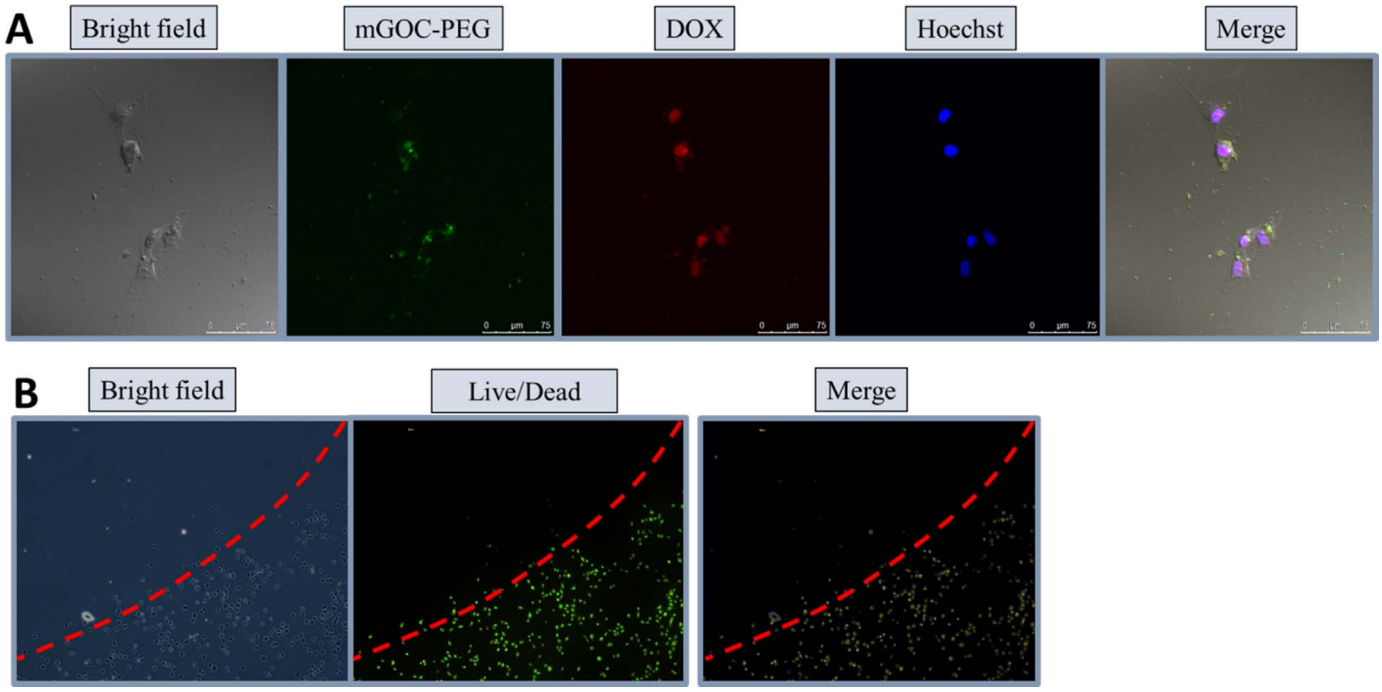

Fig. 6. (A) Cellular uptake of mGOC-PEG/DOX as examined by confocal microscopy. mGOC-PEG was labeled with fluorescein for green fluorescence. U87 cells were incubated with mGOC-PEG-carboxylfluorescein/DOX for 3 h. The nuclei are countered stained with Hoechst 33342 for blue fluorescence. Bar=75 μm. (B) The magnetic targeting study with U87 cells. The red dotted line represents the boundary of the magnet. U87 cells were treated with mGOC-PEG/DOX for 24 h and stained for live cells with a Live/Dead viability/cytotoxicity kit for mammalian cells. (For interpretation of the references to color in this figure legend, the reader is referred to the web version of this article.)

7.4 may be caused by weakening of hydrogen bonds between the drug and mGOC-PEG. Noncovalent attachment of drug to mGOC-PEG involves hydrogen bonds between –COOH of mGOC-PEG and –OH of the drug, and between –OH of mGOC-PEG and –OH of the drug. The degree of hydrogen bond interactions between the drug and mGOC-PEG is a function of pH. Under acidic condition at pH 5.4, the H^+ in solution would compete with the hydrogen bond-forming group and weaken the hydrogen bond interactions, leading to the higher rate and extent of drug release. The pH-sensitive drug release could facilitate mGOC-PEG to release its drug cargo in the acidic (pH < 6) endosomal environment after cellular uptake and increase the cytotoxicity toward cancer cells. The higher drug loading and the more pH-sensitive release of DOX suggest that mGOC-PEG is a promising delivery vehicle for the anticancer drug DOX, which will be studied in following cell culture experiments.

3.3. In vitro cellular uptake and cytotoxicity of mGOC-PEG/DOX on U87 cells

For cellular uptake of DOX-loaded nanocarrier, mGOC-PEG was first covalently conjugated with carboxylfluorescein for tracing the nanocarrier and loaded with DOX as before. After 3 h treatment of U87 cells with mGOC-PEG-carboxylfluorescein/DOX, the confocal images indicate the red fluorescence due to DOX was found mostly confined within the nuclei of shrunken cells that were stained blue with Hoechst dye (Fig. 6A). On the other hand, the green fluorescence of fluorescein-labeled mGOC-PEG appears in the cytoplasm of shrunken cells (Fig. 6A). This provides a direct evidence for endocytosis of mGOC-PEG, which accumulated in the cytoplasm after internalization. That red fluorescence was only observed in the cell nucleus indicates DOX released from mGOC-PEG in the cytoplasm can translocate across the nuclear membrane to interact with DNA molecules in the cell nucleus. Taken together, the results suggest that mGOC-PEG/DOX could be

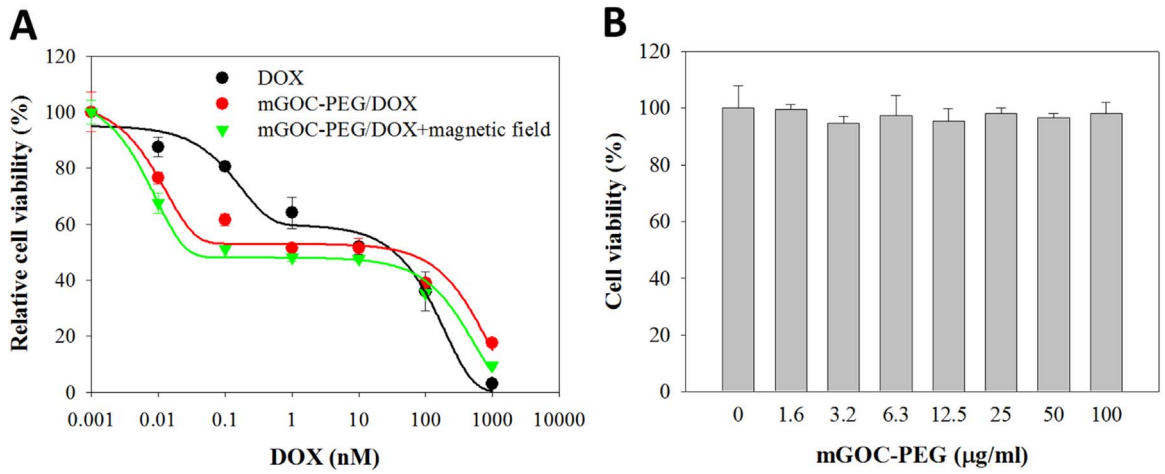

Fig. 7. (A) In vitro cytotoxicity of DOX, mGOC-PEG/DOX and mGOC-PEG/DOX+magnetic field toward U87 cells. Cell viability of U87 cells after different treatment after 24 h was determined by MTT assays. Cell viabilities with cell culture medium and mGOC-PEG were taken as 100% for DOX and mGOC-PEG/DOX, respectively. (B) Biocompatibility of mGOC-PEG toward U87 cells. Cell viabilities in the presence of different concentrations of mGOC-PEG were determined and normalized with the cell viability in cell culture medium.

transported across cell membrane via endocytosis and DOX was subsequently released under acidic intracellular environment [21].

For magnetic targeting effect, U87 cells were treated with mGOC-PEG/DOX in a 24-well culture plate that has a small permanent magnet placed at the center of the well. As can be seen from Fig. 6B, no viable cells could be found in the magnetic targeted area in the well (top to the red dotted line) after LIVE/DEAD staining. Indeed, the cytotoxicity of DOX released from mGOC-PEG/DOX will lead to cell death and dead cells will be detached from the well surface without emitting any green fluorescence signal. In contrast, abundant live U87 cells were found to attach to the well surface in the non-magnetic targeted area (bottom to the red dotted line). The mGOC-PEG/DOX could be therefore be magnetic targeted to the tumor site with a magnetic field for specific killing of cells at the targeting site with minimum side effects toward surrounding healthy cells.

Fig. 7A shows the cytotoxicity of free DOX, mGOC-PEG/DOX and mGOC-PEG/DOX + magnetic field at different DOX concentrations toward U87 cells. When treated with an equivalent concentration of DOX, U87 cancer cells show similar IC50 value for free DOX and mGOC-PEG/DOX at ~32 nM. However, the IC50 value for mGOC-PEG/DOX+magnetic field was drastically reduced to 0.03 nM. This result is consistent with the magnetic targeting study results in Fig. 6B with minimum live cells at the targeted site. Combining with the efficient cellular uptake of mGOC-PEG/DOX by U87 shown in Fig. 6A, this result confirms magnetic guidance could efficiently guide mGOC-PEG to U87 cells to improve the its internalization and efficiently deliver the drug to the cell nucleus for cytotoxicity effects. The results in Fig. 7B confirm the biocompatibility of mGOC-PEG over a broad concentration range. The concentrations of mGOC-PEG studied in Fig. 7B also covers those used in Fig. 7A, indicating cell cytotoxicity shown by mGOC-PEG/DOX was indeed from released DOX but not from the mGOC/PEG.

Although the result from in vitro cytotoxicity toward U87 cells is encouraging, successful application of mGOC-PEG as a drug carrier for cancer treatment will need to consider the role of protein corona. It is know that once nanoparticles are injected, they will interact with biological components and surrounded by a protein corona that can trigger an immune response and affect nanoparticle toxicity and targeting capabilities [19]. At this time, it still remains unclear how to optimally modify nanoparticles for in vivo application [20]. Nonetheless, the formation and immunological response to protein corona is known to be influenced by the surface properties of the nanoparticles [21]. Our future works will address the effective physio-chemical properties of mGOC-PEG for determining protein corona and associated toxicological evaluation by analyzing protein distribution and examining in vivo responses.

4. Conclusions

Magnetic targeted chemotherapy drug delivery vehicle based on mGOC-PEG was developed in this study with demonstrated advantages such as high drug loading, pH-dependent controlled release and magnetic targeting, which can overcome the limitations of conventional GO-based drug delivery systems. At a low pH condition, typical of the environment encountered in intracellular endosome, DOX can be released efficiently from the internalized nanocarriers in the cytoplasmic region and enters the nucleus to induce cell death. By magnetic guidance, selective killing of U87 cells at the magnetic targeting site is possible as evidenced from the dramatic decrease of the IC50 value. Considering the in vitro drug delivery results, we think the application of mGOC/PEG could be extended to enhance the efficiency of cancer therapy in vivo.

Acknowledgments

This work was supported by Chang Gung Memorial Hospital (BMRP 249, CMRPD3E0271 and CMRPD3E0272).

References

[1] F. Alexis, E.M. Pridgen, R. Langer, O.C. Farokhzad, Nanoparticle technologies for cancer therapy, in: Monika Schäfer-Kortingl (Ed.)Drug Delivery, Springer, Berlin, Heidelberg, 2010, pp. 55–86.
[2] M. Upreti, A. Jyoti, P. Sethi, Tumor microenvironment and nanotherapeutics, Translational, Cancer Res. 2 (2013) 309.
[3] K.H. Bae, H.J. Chung, T.G. Park, Nanomaterials for cancer therapy and imaging, Mol. Cells 31 (2011) 295–302.
[4] A.J. Cole, V.C. Yang, A.E. David, Cancer theranostics: the rise of targeted magnetic nanoparticles, Trends Biotechnol. 29 (2011) 323–332.
[5] N. Schleich, C. Po, D. Jacobs, B. Ucakar, B. Gallez, F. Danhier, V. Préat, Comparison of active, passive and magnetic targeting to tumors of multifunctional paclitaxel/SPIO-loaded nanoparticles for tumor imaging and therapy, J. Control. Release 194 (2014) 82–91.
[6] P.K. Singal, N. Iliskovic, Doxorubicin-induced cardiomyopathy, N. Engl. J. Med. 339 (1998) 900–905.
[7] T. Ikegami, Y. Matsuzaki, M. Al Rashid, S. Ceryak, Y. Zhang, B. Bouscarel, Enhancement of DNA topoisomerase I inhibitor–induced apoptosis by ursodeoxycholic acid, Mol. Cancer Ther. 5 (2006) 68–79.
[8] Z. Liu, J.T. Robinson, S.M. Tabakman, K. Yang, H. Dai, Carbon materials for drug delivery & cancer therapy, Mater. Today 14 (2011) 316–323.
[9] L. Feng, Z. Liu, Graphene in biomedicine: opportunities and challenges, Nanomedicine 6 (2011) 317–324.
[10] Z. Liu, X. Sun, N. Nakayama-Ratchford, H. Dai, Supramolecular chemistry on water-soluble carbon nanotubes for drug loading and delivery, ACS Nano 1 (2007) 50–56.
[11] X. Sun, Z. Liu, K. Welsher, J.T. Robinson, A. Goodwin, S. Zaric, H. Dai, Nano-

graphene oxide for cellular imaging and drug delivery, Nano Res. 1 (2008) 203–212.
[12] A.E. Felber, M.-H. Dufresne, J.-C. Leroux, pH-sensitive vesicles, polymeric micelles, and nanospheres prepared with polycarboxylates, Adv. Drug Deliv. Rev. 64 (2012) 979–992.
[13] S. Simoes, J.N. Moreira, C. Fonseca, N. Düzgüneş, M.C.P. de Lima, On the formulation of pH-sensitive liposomes with long circulation times, Adv. Drug Deliv. Rev. 56 (2004) 947–965.
[14] W. Jiang, H.-C. Yang, S.-Y. Yang, H.-E. Horng, J. Hung, Y. Chen, C.-Y. Hong, Preparation and properties of superparamagnetic nanoparticles with narrow size distribution and biocompatible, J. Magn. Magn. Mater. 283 (2004) 210–214.
[15] Y.J. Lu, K.C. Wei, C.C. Ma, S.Y. Yang, J.P. Chen, Dual targeted delivery of doxorubicin to cancer cells using folate-conjugated magnetic multi-walled carbon nanotubes, Colloids Surf. B Biointerfaces 89 (2012) 1–9.
[16] F. Maestrelli, M. Garcia-Fuentes, P. Mura, M.J. Alonso, A new drug nanocarrier consisting of chitosan and hydoxypropylcyclodextrin, Eur. J. Pharm. Biopharm. 63 (2006) 79–86.
[17] T. Yuda, K. Maruyama, M. Iwatsuru, Prolongation of liposome circulation time by various derivatives of polyethyleneglycols, Biol. Pharm. Bull. 19 (1996) 1347–1351.
[18] Y. Zhang, N. Kohler, M. Zhang, Surface modification of superparamagnetic magnetite nanoparticles and their intracellular uptake, Biomaterials 23 (2002) 1553–1561.
[19] Y.K. Lee, E.J. Choi, T.J. Webster, S.H. Kim, D. Khang, Effect of the protein corona on nanoparticles for modulating cytotoxicity and immunotoxicity, Int. J. Nanomed. 10 (2015) 97–113.
[20] C. Corbo, R. Molinaro, A. Parodi, N.E. Toledano Furman, F. Salvatore, E. Tasciotti, The impact of nanoparticle protein corona on cytotoxicity, immunotoxicity and target drug delivery, Nanomedicine 11 (2016) 81–100.
[21] C. Gunawan, M. Lim, C.P. Marquis, R. Amal, Nanoparticle-protein corona complexes govern the biological fates and functions of nanoparticles, J. Mater. Chem. B 2 (2014) 2060–2083.